SCIENCE CHINA
Technological Sciences

December 2013 Vol.56 No.12: 2953–2963
doi: 10.1007/s11431-013-5401-4

An improved practical model for wear prediction of revolute clearance joints in crank slider mechanisms

LI Pei, CHEN Wei & ZHU AiBin*

Key Laboratory of Education Ministry for Modern Design and Rotor-Bearing System, Xi'an Jiaotong University, Xi'an 710049, China

Received September 1, 2013; accepted October 19, 2013; published online October 31, 2013

A stationary clearance link algorithm (SCLA) for calculating the reaction-force of revolute clearance joints in crank slider mechanisms is proposed in this paper. The SCLA is more efficient than other algorithms of the same accuracy. Furthermore, based on the Winkler foundation model, an unsymmetrical Winkler foundation model and a double elastic layer Winkler model are proposed. By integrating a dynamic model and the unsymmetrical Winkler foundation model with Archard wear model, an improved integrated wear prediction model is also generated. A series of experiments have been performed to compare with the predicted analysis data, and the results showed a good agreement. As a real industry application, with the double elastic layer Winkler model, the integrated wear prediction model was successfully used to predict the wear depth of the joint bearing (bimetallic bearing) for the cantilever crane of a concrete pump truck of Sany Heavy Industry.

revolute clearance joint, stationary clearance link algorithm, unsymmetrical Winkler foundation model, double elastic layer Winkler model

Citation: Li P, Chen W, Zhu A B. An improved practical model for wear prediction of revolute clearance joints in crank slider mechanisms. Sci China Tech Sci, 2013, 56: 2953–2963, doi: 10.1007/s11431-013-5401-4

Clearance, which greatly affects the dynamic behaviors of mechanisms with clearance joints [1], is common in engineering machinery due to the machining and assembly tolerance. Nowadays, wear prediction of revolute clearance joints, which is the integration of dynamics, tribology and other subjects [2], is an important method to assess the working life and performance of mechanisms. However, it is inevitable for most of the existing methods dealing with engineering problems involving clearance, such as the contact-separation status contact force model, to solve non-linear differential equations of rigid system [3–5]. Although accurate results can be obtained by these methods, the calculation is so time consuming that it is not always possible to apply these methods into real projects. For industry applications, a reasonable method must be accurate and efficient. Thus, although more and more methods, for example, the finite element method which Su et al. [6] successfully used to predict the wear depth of revolute clearance joints, are proposed for dealing with engineering problems involved clearance [7], a practical method which can be applied into industry applications is becoming more necessary.

In ref. [8], Li presented an algorithm to simplify the process of calculating reaction force. He pointed out that when the clearance is very small, the reaction force angle γ of the revolute clearance joint can be treated the same as the ideal revolute joint. By taking the reaction force angle of the ideal revolute joint as the initial condition, the reaction force of the revolute clearance joint can be solved efficiently and accurately. However, because the reaction force of the ideal revolute joint has to be calculated at first, the dynamic model with ideal revolute joints has to be built in advance. As a result, though Li's algorithm simplifies the computing process [9], it complicates the modeling process, which sig-

*Corresponding author (email: fivestars2008@qq.com)

nificantly decreases its efficiency and practicality. In order to build a practical model to accurately and efficiently solve engineering problems involving clearance, a more efficient and easier method, a stationary clearance link algorithm (SCLA) is proposed in this paper.

It has great engineering significance that Priit Podra and Soren Andersson [10] successfully used the Winkler foundation model in predicting wear. However, although Priit Podra improved the Winkler foundation model to be a 3D model, he assumed the bearing to be an ideal arc, which is obviously not true when the bearing is worn. In this paper, unsymmetrical calculation of the Winkler foundation model with changing curvature is proposed, and the results show that unsymmetrical calculation is reasonable and practical.

It is necessary to develop a practical integrated wear prediction model for real industry applications [5, 11]. In this paper, a practical wear prediction model is proposed and successfully applied to an industry application.

1 An improved practical algorithm for calculating reaction force

Wear is caused by the contact force and the relative motion of the contact pair, and the two factors both can be solved in dynamic models. However, most of the existing methods for solving dynamic models are so complex and time-consuming that they cannot be easily used to solve industry problems efficiently. In order to calculate the reaction force in dynamic models efficiently and accurately, an improved practical algorithm based on Li's algorithm [8] is proposed.

1.1 Dynamic model and equations

There are many classical models for revolute clearance joints, such as the clearance link model, the contact-separation status contact force model and so on. However, it is obvious that a complex model leads to lower computing efficiency, which must be taken into consideration in order to find out an efficient method to predict wear of revolute clearance joints in engineering applications. Comparing with the contact-separation status contact force model and other complex models, the clearance link model has much higher efficiency while its results are accurate enough for engineering applications. Thus, in this paper, the clearance link model is taken to represent revolute clearance joints.

As one of the most common mechanisms, the crank slider mechanism is frequently used in engineering machinery. The crank slider mechanism is taken as a dynamic mechanism involving a revolute clearance joint. After integrating the clearance link model with the crank slider mechanism, the dynamic model is built and shown as Figure 1, in which the clearance link CD represents the revolute clearance joint, and the spring provides load to the mechanism. Because of the existing of the clearance link, the mechanism has two

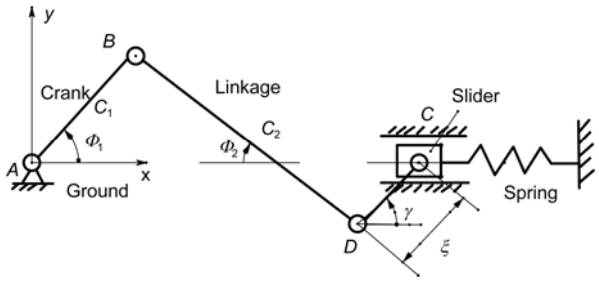

Figure 1 Crank slider mechanism with a clearance revolute joint.

degrees of freedom (DOFs) γ and Φ_1, defined as the direction angle of the clearance link and the rotation angle of the crank, respectively.

As is shown in Figure 1, the lengths of crank *AB*, linkage *BD* and clearance link *CD* are L_1, L_2, and ξ, respectively; the masses of crank *AB*, linkage *BD* and slider *C* are m_1, m_2, and *m*, respectively. The constraint equations of the crank slider mechanism are as follows:

$$L_1\cos\Phi_1 + L_2\cos\Phi_2 + \xi\cos\gamma = x_s, \tag{1}$$

$$L_1\sin\Phi_1 - L_2\sin\Phi_2 + \xi\sin\gamma = 0. \tag{2}$$

Subsequently we infer that

$$\Phi_2 = \arcsin\left(\frac{L_1\sin\Phi_1 + \xi\sin\gamma}{L_2}\right), \tag{3}$$

$$\dot{\Phi}_2 = \frac{L_1\dot{\Phi}_1\cos\Phi_1 + \xi\dot{\gamma}\cos\gamma}{\sqrt{L_2^2 - \left(L_1\sin\Phi_1 + \xi\sin\gamma\right)^2}} = \frac{L_1\dot{\Phi}_1\cos\Phi_1 + \xi\dot{\gamma}\cos\gamma}{L_2\cos\Phi_2}, \tag{4}$$

$$\ddot{\Phi}_2 = \frac{L_1\ddot{\Phi}_1\cos\Phi_1 - L_1\dot{\Phi}_1^2\sin\Phi_1 + \xi\ddot{\gamma}\cos\gamma - \xi\dot{\gamma}^2\sin\gamma + L_2\dot{\Phi}_2^2\sin\Phi_2}{L_2\cos\Phi_2}, \tag{5}$$

$$\dot{x}_s = -L_1\dot{\Phi}_1\sin\Phi_1 - L_2\dot{\Phi}_2\sin\Phi_2 - \xi\dot{\gamma}\sin\gamma, \tag{6}$$

$$\ddot{x}_s = -L_1\ddot{\Phi}_1\sin\Phi_1 - L_1\dot{\Phi}_1^2\cos\Phi_1 - L_2\ddot{\Phi}_2\sin\Phi_2 - L_2\dot{\Phi}_2^2\cos\Phi_2 - \xi\ddot{\gamma}\sin\gamma - \xi\dot{\gamma}^2\cos\gamma. \tag{7}$$

According to the principle of D'Alembert,

$$F_{Cx}^{'} - m_3\ddot{x}_3 + F_s = 0, \tag{8}$$

$$F_{Cx}^{'} = -F_{Cx}, \tag{9}$$

$$F_{Cy}(x_C - x_B) - F_{Cx}(y_C - y_B) + \left(-m_2\ddot{y}_2 - m_2 g\right)(x_2 - x_B) - \left(-m_2\ddot{x}_2\right)(y_2 - y_B) + I_B\ddot{\Phi}_{BC} = 0, \tag{10}$$

where I_B is the moment of inertia of the linkage wrt point *B*, F_{Cx} is the reaction force of the revolute clearance joint along the *x* axis and F_{Cy} along the *y* axis.

With simultaneous eqs. (3)–(10), it is obvious that if the direction angle γ of the clearance link is known, the reaction force of the revolute clearance joint can be solved.

In addition, the relation between the direction angle of the clearance link γ and the reaction force of the revolute clearance joint can be formulated as follows:

$$\gamma = \arctan\frac{F_{Cy}}{F_{Cx}}, \tag{11}$$

$$\dot{\gamma} = \frac{F_{Cx}\dot{F}_{Cy} - F_{Cy}\dot{F}_{Cx}}{F_{Cx}^2 + F_{Cy}^2}, \tag{12}$$

$$\ddot{\gamma} = \frac{F_{Cx}\ddot{F}_{Cy} - F_{Cy}\ddot{F}_{Cx}}{F_{Cx}^2 + F_{Cy}^2} - \frac{2\left(F_{Cx}\dot{F}_{Cx} + F_{Cy}\dot{F}_{Cy}\right)\left(F_{Cx}\dot{F}_{Cy} - F_{Cy}\dot{F}_{Cx}\right)}{\left(F_{Cx}^2 + F_{Cy}^2\right)^2}. \tag{13}$$

1.2 Stationary clearance link algorithm (SCLA)

From the dynamic equations of the crank slider mechanism with a revolute clearance joint, the reaction force of the revolute clearance joint can be solved if the direction angle γ of the clearance link is known. To avoid solving γ of the ideal revolute joint, let γ be a constant as a start point and $\dot{\gamma}$ and $\ddot{\gamma}$ be zero, which means the clearance link is stationary. The reaction force and its angle can easily be calculated with the dynamic model. Typically, the clearance is very small, the reaction force angle can be treated as the actual reaction force angle γ of the revolute clearance joint. By substituting the new γ back into the dynamic model, the reaction force of the revolute clearance joint can be finally computed. The flowchart of the stationary clearance link algorithm (SCLA) is shown in Figure 2.

1.3 Numerical simulation of reaction force

In order to illustrate the accuracy and efficiency of the SCLA, the parameters of the crank slider mechanism are assumed as in Table 1.

As the initial condition γ is an undetermined constant, different initial conditions are utilized to calculate the reaction force for understanding the influence of the initial condition on the results of the SCLA. The comparison of the results is shown in Figure 3.

As shown in Figure 3, the influence of the initial condition on the results of the SCLA is small enough to be ignored, which means any initial conditions can be used in the SCLA.

In order to prove the accuracy of the SCLA, the results solved by SCLA and Li Zhe's algorithm are compared, which is shown in Figures 4 and 5. In Figure 4, RFCJ and RFIJ respectively mean the reaction forces of the clearance joint and the ideal joint.

Figures 4 and 5 indicate that results of reaction forces calculated by the SCLA and Li Zhe's algorithm are almost identical, and the differences between two results can be ignored in ideal projects. Hence, the result calculated by SCLA is accurate.

The SCLA has not only good accuracy but also high efficiency because of not modeling and solving of the ideal revolute joint. The computation times of the SCLA and Li

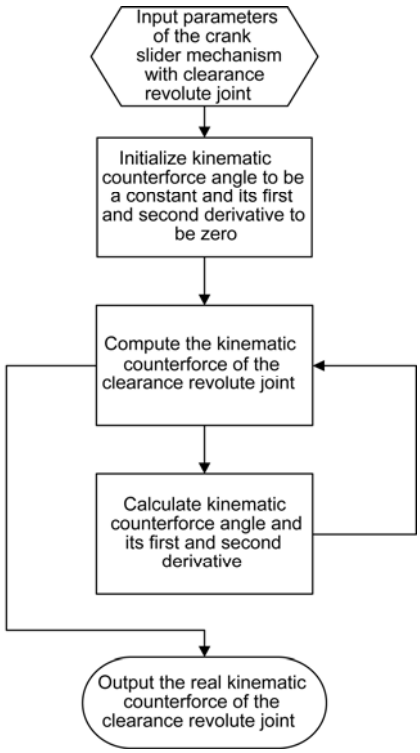

Figure 2 Flowchart of the SCLA.

Table 1 Parameters of the crank slider mechanism

L_1 (mm)	L_2 (mm)	ξ (mm)	m_1 (kg)	m_2 (kg)	m_3 (kg)	k (N/m)
70	200	0.05	0.462	1.0943	5.000	0

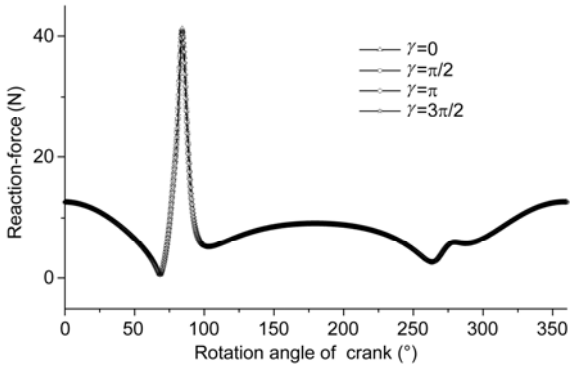

Figure 3 Results of reaction forces calculated with different initial conditions by SCLA.

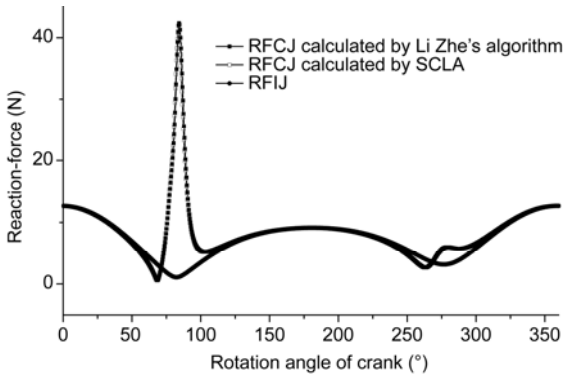

Figure 4 Results of reaction forces calculated by different algorithms.

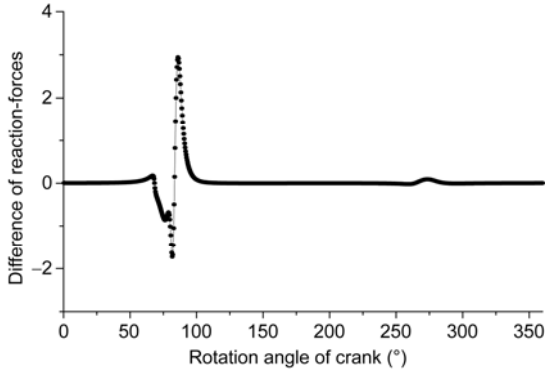

Figure 5 Difference of reaction forces calculated by the two algorithms.

Zhe's algorithm are shown in Table 2.

As shown in Table 2, compared with Li Zhe's algorithm, the efficiency of SCLA is more than 20 times higher. In real projects, the reaction force usually needs to be calculated for thousands or even million cycles. Thus, the enormous improvement of efficiency made by the SCLA would have significant value in practical applications. Furthermore, because of not modeling and solving of the ideal revolute joint, the SCLA is much simpler and easier in programming, which makes the SCLA more suitable in practical applications.

2 Winkler foundation model for computing the pressure distribution

In wear prediction of revolute clearance joints, real-time calculations of the pressure distribution are usually difficult to deal with. Nowadays, one of the most powerful analysis methods is the finite element method (FEM) [6, 12–14]. Whereas the FEM is often time-consuming so that the application of the FEM is still constrained by its efficiency. In order to find an efficient way to predict wear of revolute clearance joints in engineering applications, it is necessary to utilize a time-saving method in calculating the pressure distribution. Thus, the Winkler foundation model is usually adopted and discussed in real projects.

2.1 Unsymmetrical calculation with Winkler foundation model

In analysis of revolute joints, the Winkler foundation model is frequently used because of its efficiency and simplicity. However, in most of the studies, the revolute joint is throughout treated as ideal circles when calculating the pressure distribution. Obviously, the curvature of the joint changes when the joint is worn, which means the revolute joint cannot be regarded as ideal circles [6]. To be consistent with the actual situation, an improved Winkler model is proposed for bushings with continuously changing curvature.

As shown in Figure 6, if the revolute clearance joint is persistently treated as ideal cycles, the deformation of the bushing caused by the pin under an external force F is symmetrical along the external force direction. However, when considering the wear of the bushing, the bushing's inner profile is not an ideal circle. As a result, the deformation of the bushing caused by the pin under an external force F becomes unsymmetrical along the external force direction.

As the same with the traditional Winkler foundation model, in order to simplify the calculation and increase the efficiency, it is assumed that only one of the contact bodies is deformable, then the contact pressure for any spring can be formulated as [10]

$$p_i = \frac{E_w}{L_i}\delta_i, \tag{14}$$

in which p_i is the contact pressure, L_i is the thickness of the foundation layer, δ_i is the deformation of the spring, and E_w is the equivalent elastic modulus of the foundation layer. According to ref. [10], E_w is determined by

$$E_w = \frac{(1-\nu)E}{(1+\nu)(1-2\nu)}, \tag{15}$$

Table 2 Computation times of the two algorithms

Computer configuration				Computation time (1 cycle)	
CPU	RAM	System	Software	Li Zhe's Algorithm	SCLA
AMD Athlon(tm) II X2 215 Processor 2.70 GHz	3 GB (2.75 GB Available)	Windows 7 Ultimate	Matlab R2012a	0.099 s	0.0046 s

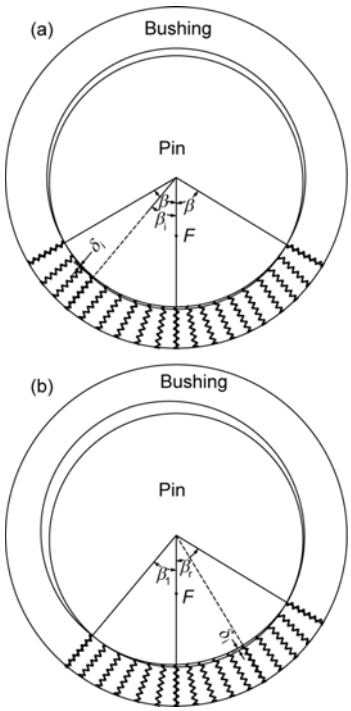

Figure 6 (a) Revolute clearance joint represented by traditional Winkler foundation model; (b) Revolute clearance joint represented by unsymmetrical Winkler foundation model.

where E and ν are the elastic modulus and the Poisson's ratio of the foundation layer, respectively.

According to Newton's law, along the external force direction, the forces are equilibrium, thus

$$F = \sum p_i A_i \cos \beta_i, \tag{16}$$

where A_i is the contact area of the spring i, β_i is the angle between the external force direction and the spring i.

In the traditional Winkler foundation model, the number of deformed springs on the left and right sides of the load direction are the same, which means the total number of deformed springs is calculated as

$$N = 2 \times N_l \quad \text{or} \quad N = 2 \times N_r, \tag{17}$$

where N is the total number of deformed springs, N_l and N_r are separately the numbers of deformed springs on the left and right sides of the load direction, and $N_l = N_r$. And deformations and pressures of deformed springs on the left and right sides of the load direction are symmetrical.

Differently, in the unsymmetrical Winkler foundation model, in order to adapt to curve surfaces with continuous curvature, calculation of the number of deformed springs and the contact pressures should be unsymmetrical along the external force direction. Thus $N_l \neq N_r$, and the total number of deformed springs is calculated as

$$N = N_l + N_r, \tag{18}$$

where the symbolic meanings are the same as eq. (17). And as a result, deformations and pressures of deformed springs on the left and right sides of the load direction are computed unsymmetrically.

2.2 Numerical simulation of pressure distribution

With regard to a revolute clearance joint, it will be worn more and more seriously, which makes the curvature of the bushing's inner profile change more and more severely. Thus, along with the increase of the joint's working time, the asymmetry of the pressure distribution becomes more and more obvious. An example is illustrated to demonstrate the improved Winkler foundation model. The parameters of the revolute clearance joint are shown in Table 3.

The load of the revolute clearance joint is provided by the reaction force in the crank slider mechanism (Figure 1). All the parameters of the crank slider mechanism are the same as Table1 except changing the spring constant to 1800 N/m (the spring constant is for accelerating the wear of the revolute clearance joint). The load is shown in Figure 7.

With the load shown in Figure 7, the pressure distribution of the elastic layer is separately solved with the traditional Winkler foundation model and the unsymmetrical Winkler foundation model. The results are separately shown in Figures 8 and 9, in which X axis represents the circumferential direction, and Y axis is the rotation step of the specified cycle appointed in titles of the Figures.

Figure 8 shows that the pressure distribution calculated

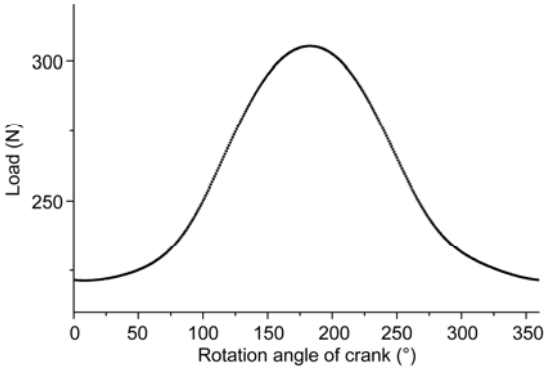

Figure 7 Load of the revolute clearance joint.

Table 3 Parameters of the revolute clearance joint

Diameter of pin (mm)	Inner diameter of bushing (mm)	Thickness of bushing (mm)	Width of bushing (mm)	Material of pin	Material of bushing
14.9	15	0.5	28	Steel (E=208 GPa, ν=0.28)	PTFE (E=0.5 GPa, ν=0.3)

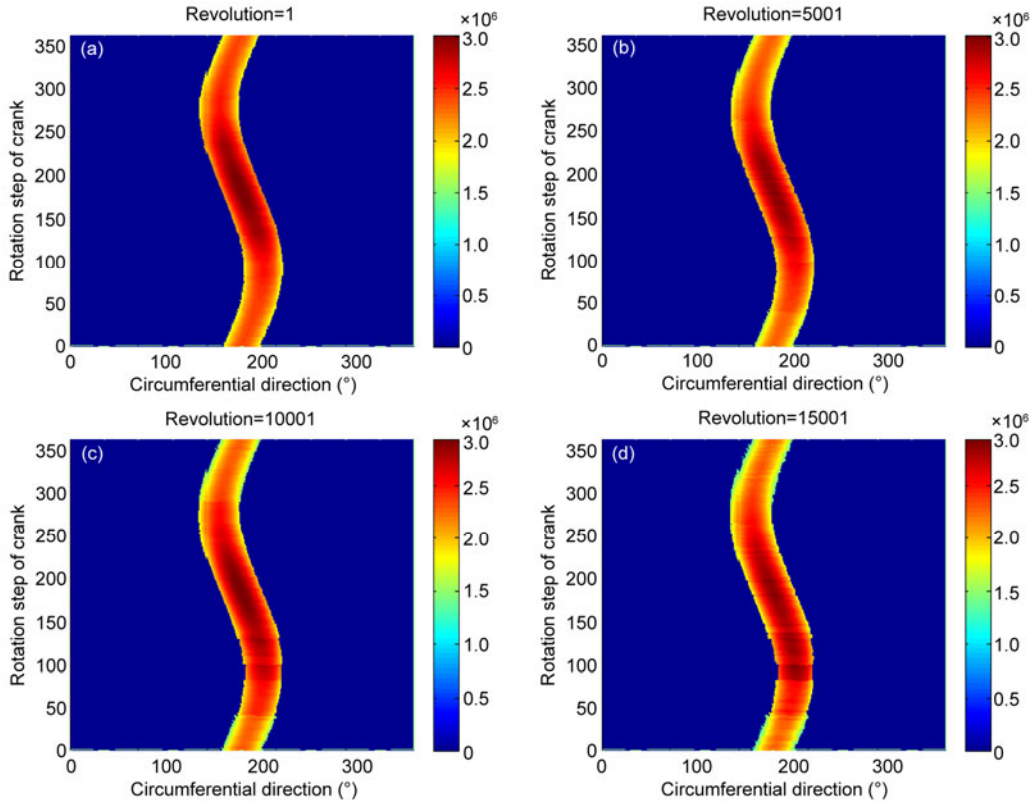

Figure 8 Pressure distributions of the revolute clearance joint calculated with traditional Winkler model. (a) Revolution=1; (b) revolution=5001; (c) revolution=10001; (d) revolution=15001.

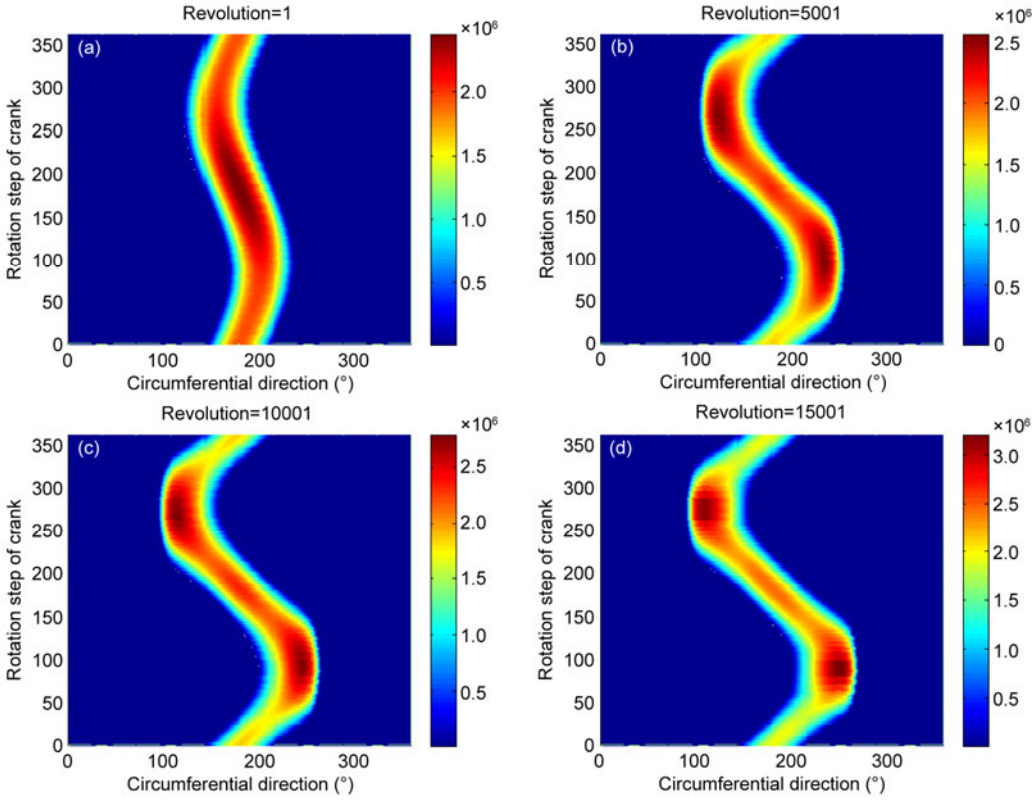

Figure 9 Pressure distributions of the revolute clearance joint calculated with improved Winkler model. (a) Revolution=1; (b) revolution=5001; (c) revolution=10001; (d) revolution=15001.

with the traditional Winkler model is always symmetrical no matter what the wear revolution is. However, this kind of pressure distribution is unreasonable because the traditional Winkler foundation model persistently treats the arc line under contact as an ideal circular arc. And it is obvious that with the traditional Winker model, the wear area does not expand, which is obviously illogical.

Different from the traditional Winkler foundation model, in the unsymmetrical Winkler foundation model, when the revolute clearance joint is not worn, the pressure distribution in any step of one cycle is symmetrical (Figure 9(a)), but when the revolute clearance joint is worn after working for several revolutions, the pressure distributions of the steps near 90th and 270th steps are obviously unsymmetrical (Figures 9(b), (c), (d)). And the results show that with the wear revolution increasing, the asymmetry of the pressure distribution becomes more and more severe. Interestingly, the most severe asymmetry of the pressure distribution approximately appears at the 90th and 270th steps, which is the boundary of wear area (shown in the *X* axis), and this leads to the expanding of the wear area.

It is important that the computing time of the unsymmetrical calculation is just about two times of that of the traditional Winkler model while the unsymmetrical Winkler model can be used for curve surfaces with changing curvature.

3 Wear prediction model: The integration of the dynamic model and the unsymmetrical Winkler foundation model with Archard wear model

For predicting the wearing depth, besides the dynamic model and the unsymmetrical Winkler foundation model, a model for calculating wear depth with the calculated pressure and relative displacement is indispensable. Nowadays, there are many models for wear calculation, but most of them aim at special situations. In this paper, considering the models' practical applicability, the Archard wear model, which has good applicability and recognition, is chosen out.

3.1 Archard wear model

The Archard wear model can be formulated as

$$\frac{V}{S} = K\frac{F_N}{H}, \tag{19}$$

where V is the wear volume, S is the relative sliding distance of the contact interfaces, K is the coefficient of wear, F_N is the normal load of the contact interfaces and H is Brinell Hardness.

As the wear depth is of more interest than the wear volume, eq. (19) can be rewritten as [10]

$$h = \frac{K}{H}pS, \tag{20}$$

where h is the wear depth and p represents the normal contact pressure. After differentiation, eq. (20) can be written as

$$\frac{\mathrm{d}h}{\mathrm{d}S} = K\frac{p}{H} = K_d p, \tag{21}$$

where K_d is the linear coefficient of wear, which is usually assigned according to experimental data. After discretizing the wear process into several steps, the cumulative wear depth in step i is the sum of the cumulative wear depth in step i–1 and the wear depth in step i, which is formulated as

$$h_i = h_{i-1} + \mathrm{d}h_i = h_{i-1} + K_d p_i \mathrm{d}S_i. \tag{22}$$

As the wear process is very slow, the wear depth of one revolution nearly has no influence on the contact faces, so the wear depth of each revolution in several continuous revolutions can be regarded as the same, which means the wear depth of several continuous revolutions can be taken as an amplification of the wear depth of one revolution. If we mark the amplification coefficient as M, eq. (22) is transformed into

$$h_i = h_{i-M+1} + \mathrm{d}h_i = h_{i-M+1} + MK_d p_i \mathrm{d}S_i. \tag{23}$$

3.2 Integrated wear prediction model

The process of the predicting model can be described as follows.

1) Calculate the relative sliding distance and the reaction force of revolute clearance joints with the dynamic model.

2) Asymmetrically compute the pressure distribution of revolute clearance joints by the unsymmetrical Winkler foundation model with the reaction force results.

3) Calculate the wear depth by Archard wear model with the pressure distribution and the relative sliding distance.

4) Update the outline of revolute clearance joints with the wear depth, and judge whether the calculation should be stopped. If the calculation should be stopped, then the program outputs the wear depth, or the program keeps working in the loop.

The flowchart of the wear prediction model is shown in Figure 10.

3.3 Numerical simulation and experimental validation

In order to test and verify the integrated wear prediction model, series of experiments were done with an experiment rig of crank-slider mechanism, and corresponding numerical simulations were also calculated.

The experiment rig is shown in Figure 11. Figure 11(a) is the 3D model and Figure 11(b) is the photo of the experiment

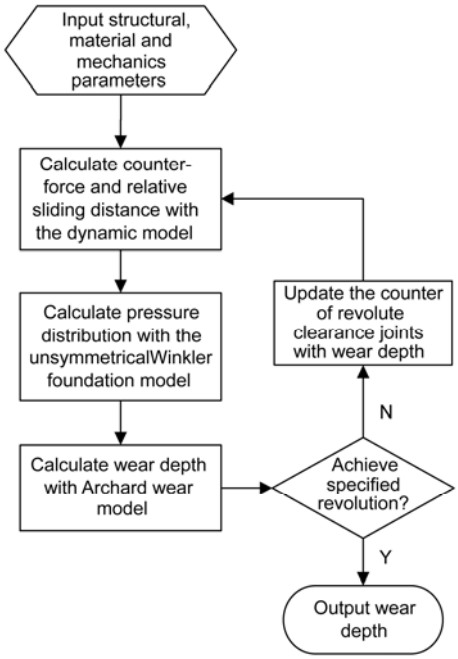

Figure 10 Flowchart of the integrated prediction model.

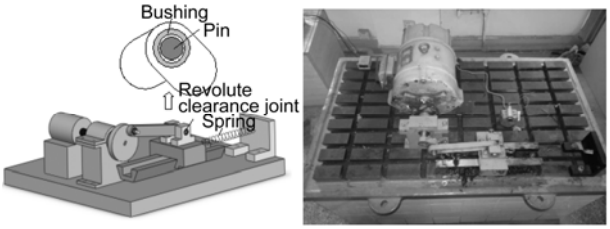

Figure 11 Experiment rig. (a) 3D model; (b) photo.

rig. Parameters of the experiment rig are the same as Table 1 except changing the spring constant to 1009.4 N/m (measured before experiment). Parameters of the revolute clearance joint in the experiment rig are the same as Table 3.

The controllable experiment parameters are the rotate speed of crank, the revolution of crank and the clearance size, and variable-controlling approach is used in our experiments. The wear depths of the revolute clearance joints are measured with an optical profiler.

When setting the speed of crank to 276 r/min, the prediction data and the experiment data of the wear depth with different revolutions (clearance size is 0.05 mm) are shown in Figure 12 (in which (a) is the result of rotating for 10000 revolutions and (b) is for 15000 revolutions). The prediction computing times were 9 s for (a) and 12 s for (b).

When setting the revolution of crank to 10000 revolutions, the prediction data and the experiment data of the wear depth with different rotate speeds (clearance size is 0.05 mm) are shown in Figure 13 (in which (a) is the result for rotate speed of 148 r/min and (b) is for 276 r/min). The prediction computing times were both 9 s.

After changing the structural parameters of bearings to change the clearance size and setting rotate speed and revolution of crank to 230 r/min and 10000 revolutions, the prediction data and the experiment data of the wear depth with different clearance sizes are shown in Figure 14 (in which (a) is the result for clearance of 0.1 mm and (b) is for 0.15 mm). The prediction computing times were both 9 s.

With the series of the experiment data and the prediction data of the wear depth, it can be obviously obtained that the prediction data coincides with the experiment data very well when considering machining, assembly and measuring tolerances.

Importantly, the integrated wear prediction model is greatly efficient. In predicting the wear depth of an experiment, the integrated wear prediction model just needed less than half a minute while the FEM (finite element method) needed several hours. In practical applications, accuracy and efficiency usually determine whether a theoretical method can be used or not. Obviously, the integrated wear prediction model in this paper is accurate and efficient enough to be usable in real projects.

4 Practical application of wear prediction model

The integrated wear prediction model was used to predict the wear depth of the joint bearing in the cantilever crane of a concrete pump truck (Figure 15).

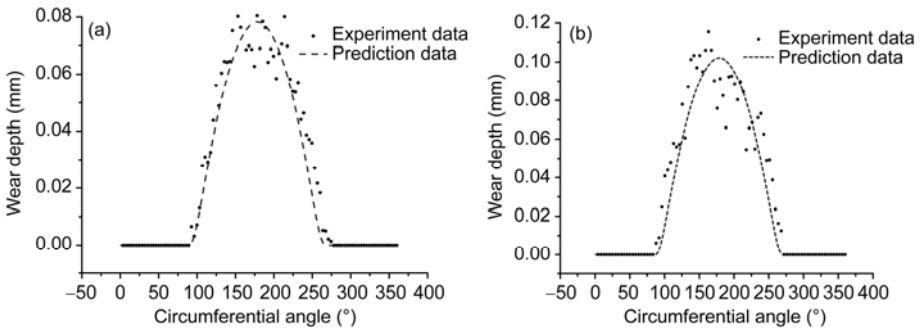

Figure 12 Experiment data and prediction data of wear depth (clearance=0.05 mm, rotate speed=276 r/min). (a) Revolution=10000; (b) revolution=15000.

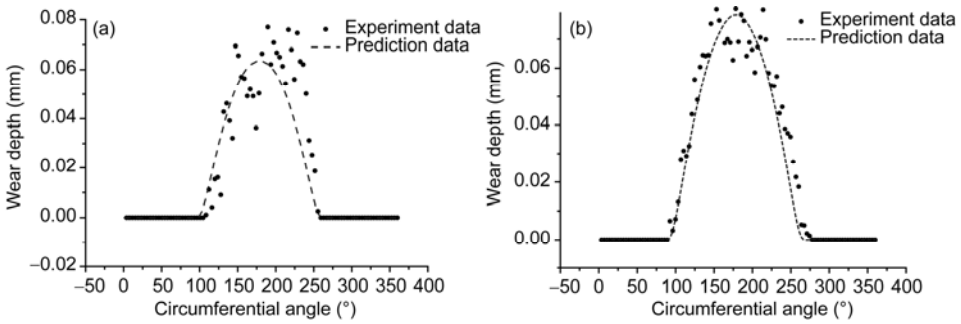

Figure 13 Experiment data and prediction data of wear depth (clearance=0.05 mm, revolution=10000). (a) Rotate speed=148 r/min; (b) rotate speed=276 r/min.

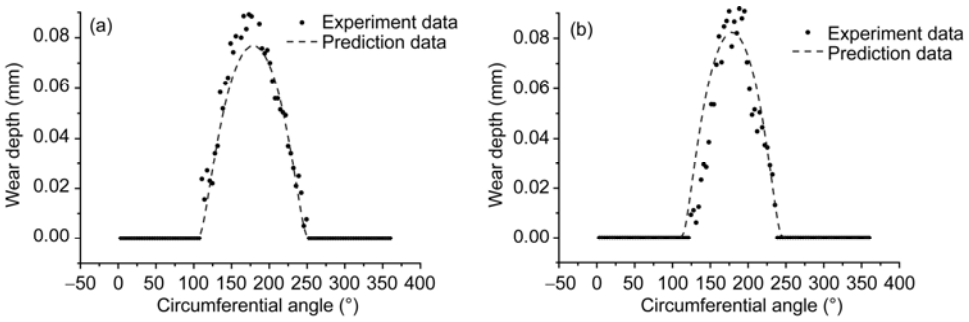

Figure 14 Experiment data and prediction data of wear depth (rotate speed=230 r/min, revolution=10000). (a) Clearance=0.1 mm; (b) clearance=0.15 mm.

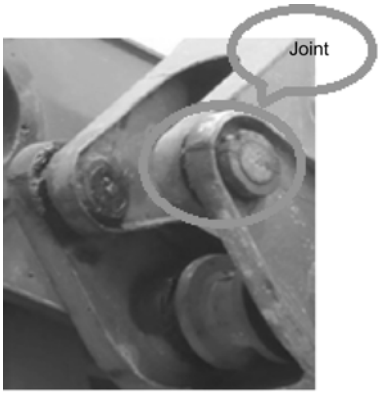

Figure 15 Joint in the cantilever crane of a concrete pump truck.

The joint bearing's working station cycled between widely swing with angular amplitude of 20 degrees for about one hour and slightly swing with angular amplitude of 1 degree for approximately 4 hours. The parameters of the joint bearing are listed in Table 4.

4.1 Double elastic layers Winkler model for bimetallic bearing

In order to apply the integrated wear prediction model in the bimetallic bearing, a double elastic layers Winkler model was created, as shown in Figure 16.

To be similar with the unsymmetrical Winkler foundation model, eqs. (14) – (16) and (18) are suitable for this model. If marking the deformation of copper layer, steel layer and the total deformation of element i as δ_i^{copper}, δ_i^{steel} and δ_i, then

$$\delta_i = \delta_i^{\text{copper}} + \delta_i^{\text{steel}}, \tag{24}$$

and because of the balance of forces, it is obvious that

$$F_i = \frac{E_w^{\text{copper}}}{L_i^{\text{copper}}} \delta_i^{\text{copper}} A_i^{\text{copper}} \cos\beta_i = \frac{E_w^{\text{steel}}}{L_i^{\text{steel}}} \delta_i^{\text{steel}} A_i^{\text{steel}} \cos\beta_i, \tag{25}$$

where E_w^{copper} and E_w^{steel} are respectively the equivalent

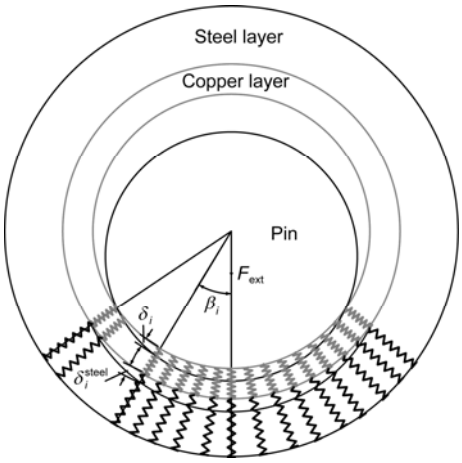

Figure 16 Double elastic layers Winkler model.

Table 4 Parameters of the joint bearing in the cantilever crane of the concrete pump truck

Diameter of pin	Inner diameter of bushing	Width of bushing	Thickness of steel layer	Thickness of copper layer	Material of pin	Material of steel layer	Material of copper layer
14.9 mm	15 mm	28 mm	2 mm	0.5 mm	Steel (E=208 GPa, ν=0.28)	Steel (E=208 GPa, ν=0.28)	Copper (E=103 GPa, ν=0.3)

elastic moduli of the copper layer and the steel layer, L_i^{copper}, A_i^{copper}, L_i^{steel} and A_i^{steel} are separately the thickness and the contact area of the copper layer and the steel layer in element i.

After replacing the Winkler foundation model with the double elastic layer Winkler model in the integrated wear prediction model, the wear depth of the joint bearing in the cantilever crane of the concrete pump truck can be predicted.

4.2 Results of predicted and actual wear depth

The actual wear depth data, shown in Figure 17(a), was provideed by Sany Heavy Industry. After filtering processing, the actual wear depth data is shown in Figure 17 (b).

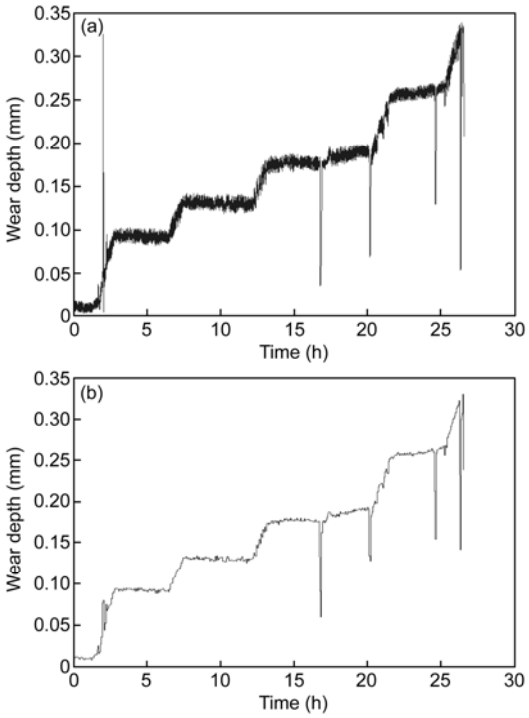

Figure 17 Actual wear depth data. (a) Original data; (b) data after filtering.

The joint bearing's working status can be divided into phases, and each phase includes about 5 hours. This phased feature is confirmed in the actual wear depth data (Figure 17). With the improved integrated wear prediction model, the prediction wear depth data was calculated and compared with the actual wear depth data in Table 5. In addition, in Table 5, the computing time of our model is also listed.

Table 5 indicates that the predicted wear depth is smaller than the actual wear depth, but the relative error is small enough to be tolerated in practical applications. The error originates from machining error, assembly error, measuring error and discretization error. From Table 5, it can be obtained that along with the increase of wear time, the relative error of the predicted wear depth decreases. Besides, the computing time of the whole prediction process is less than a minute. The wear prediction model proposed in this paper is validated to be practical, feasible, accurate and efficient.

5 Conclusions

1) In this paper, a stationary clearance link algorithm (SCLA) is proposed for calculating the reaction force of revolute clearance joints in crank slider mechanisms. Compared with other algorithms, the efficiency of the SCLA is more than 20 times higher, and because of not modeling and solving of ideal revolute joints, the SCLA is much simpler and easier in programming, which makes the SCLA more suitable in practical applications.

2) An unsymmetrical Winkler foundation model is proposed for the worn revolute clearance joint with continuously changing curvature. The results of the unsymmetrical Winkler foundation model obviously show the asymmetry of the pressure distribution and effectively explain the expanding of the wear area.

3) After integrating the dynamic model and the unsym-

Table 5 Results of predicted and actual wear depth

Phase	Actual wear depth (mm)	Predicted wear depth (mm)	Relative error	computing time (s)
1st (5 h)	0.094	0.076	19.1%	2.8
2nd (10 h)	0.130	0.123	5.4%	4.9
3rd (15 h)	0.176	0.167	5.1%	6.8
4th (20 h)	0.214	0.209	2.3%	8.8
5th (25 h)	0.253	0.252	0.4%	11.0

metrical Winkler foundation model with the Archard wear model, an integrated wear prediction model is proposed. With the integrated wear prediction model, the wear depth of the revolute clearance joint in the experiment rig was successfully predicted. The comparison of the prediction data and the experiment data shows that the integrated wear prediction model is accurate and efficient.

4) With the double elastic layer Winkler model, the integrated wear prediction model was used to predict the wear depth of the joint bearing (a bimetallic bearing) in the cantilever crane of the concrete pump truck. The good agreement was achieved between the predicted wear depth data and the actual wear depth data measured by Sany Heavy Industry, which indicates that the integrated wear prediction model is accurate and efficient enough to be utilized in real industry application

This work was supported by the National Natural Science Foundation of China (Grant No. 51175409).

1 Liu Y C, Yu Y Q. A survey of mechanism and Robot with clearances. Mech Sci Tech, 2004, 23 (4): 454-457
2 Xie Y B. Three axioms in tribology. Tribology, 2001, 21(3): 161–165
3 Flores P, Ambrosio J. Revolute joints with clearance in multibody systems. Comput Struct, 2004, 82: 1359–1369
4 Imed K, Lotfi R. Dynamic analysis of a flexible slider-crank mechanism with clearance. European J Mecha A/Solids, 2008, 27: 882–898
5 Sfantos G K, Aliabadi M H. Wear simulation using an incremental sliding Boundary Element Method. Wear, 2006, 260 (9-10): 1119–1128
6 Su Y W, Chen W, Xie Y B. Intergrated Analysis Between Tribology and Dynamics in Multibody System with Clearance Revolute Joints and Its Application. Dissertation of Doctoral Degree. Xi'an: Xi'an Jiaotong University, 2010
7 Wen S Z, Huang P. Principles of Tribology. 3rd ed. Beijing: Tsinghua University Press, 2008
8 Li Z, Li L, Bai S X. A new method of predicting the occurrence of contact loss between pairing elements in planar linkages with clearances. Mech Machine Theory, 1992 , 27 (3): 295–301
9 Zhang J F, Xu Q Y, Zhang L. The algorithm for the clearance joint reaction force of slider-crank mechanism and its application. Chinese J Appl Mech, 2001, 18(4): 93–97
10 Podra P, Andersson S. Wear simulation with the Winkler surface model. Wear, 1997, 207: 79–85
11 Wen S Z. Existing state and development of tribology research in China. Chinese J Mech Eng, 2004, 40(11): 1–6
12 Podra P, Andersson S. Simulation sliding wear with finite element method. Tribology Inter, 1999, (32): 71–81
13 Podra P, Andersson S. Finite element analysis wear simulation of a conical spinning contact considering surface topology. Wear, 1999, 224: 13–21
14 Bandeira A A, Wriggers P, Pimenta P. Numerical derivation of contact mechanics interface laws using a finite element approach for large 3D deformation. Int J Meth Engng, 2004, 59: 173–195
15 Flodin A, Andersson S. Simulation of mild wear in spur gears. Wear, 1997, 207: 16–23
16 An K N, Himenso S, Tsumura H, et al. Pressure distribution on articular surfaces-application to joint stability evaluation. J Biomech, 1990, 23(10): 1013–1020